06

Applicability of XANES spectroscopy and machine learning methods for the determination of local atomic structure of Cu-MOR zeolites

© Ya.N. Gladchenko-Djevelekis, G.B. Sukharina, A.M. Ermakova, K.D. Kulaev, V.V. Pryadchenko, E.E. Ponosova, E.I. Shemetova, L.A. Avakyan, L.A. Bugaev

Southern Federal University,
344090 Rostov-on-Don, Russia
e-mail: ygl@sfedu.ru, gbsukharina@sfedu.ru

Received November 16, 2023
Revised December 31, 2023
Accepted January 26, 2024

The research is devoted to the development of methods of the determination of the local structure of copper centers in Cu-MOR using a combination of machine learning and X-ray absorption spectroscopy techniques. Cu-zeolites are promising catalysts for processes of environmentally friendly production of methanol from natural methane gas, the catalytic activity of which is mostly determined by the local environment of copper atoms in the zeolite. The irregular distribution of copper centers in the zeolite framework increases the complexity of the problem, since it makes difficult to interpret the experimental Cu *K*-XANES spectra. Machine learning algorithms trained on the synthetic data obtained in the FDMNES software package allowed us to determine the location of copper centers in a particular zeolite ring with an accuracy of 0.97 according to the F1 metric.

Keywords: zeolites, atomic structure, XANES, ML-classification, neural networks.

DOI: 10.61011/JTF.2024.04.57533.287-23

Introduction

Zeolites are microporous aluminosilicate compounds that are used commercially as catalysts. For example, zeolites are being examined and optimized in C1 chemistry for application in the process of conversion of methane into methanol. The presence of active centers containing atoms of transition metals [1–5] is the cause of a high catalytic activity of zeolites. It is difficult to examine the structure of catalytically active centers in detail, since the distribution of such centers in the zeolite framework is nonuniform and is affected by a variety of interrelated factors (e.g., the molar ratio of reagents in the process of synthesis, reaction time and temperature, etc.) [6–9]. Thus, the production of efficient catalysts involves the study of specific structural parameters of metallic centers and their effect on catalytic properties. Systematic studies of this kind have not been performed yet [10] and require refinement of the existing approaches.

Machine learning (ML) techniques are a promising tool for determination of the structure of various materials [11–13] (zeolites included), since they allow one to perform calculations for nonlinear or massively combinatorial processes that cannot be probed by conventional approaches [14]. Considering the vast number of factors shaping the structure in synthesis of zeolites and the variety of types of copper centers affecting their catalytic properties, the use of ML is especially timely for improving zeolite synthesis. The application of ML in this field should provide an opportunity to automate and simplify the process of determination of structural characteristics of zeolites based on experimental data for the purpose of identifying the laws of influence of structural features of zeolites on their catalytic properties [15]. The study where the elastic response of pure silica zeolites was predicted by ML [16] is a well-documented example of this. The authors used a gradient boosting regressor (GBR) [17,18] and a training set of elastic properties calculated by density functional theory (DFT). It turned out that the applied ML approach allows one to predict bulk and shear moduli of zeolites much faster and with an accuracy exceeding the one achieved with the use of classical interatomic pair potentials. ML was also used to predict possible intermediates of the reaction of conversion of carbon dioxide into methanol involving zeolites modified by metals [19]. XGBoost and ExtraTrees algorithms were applied in this research.

The present study is focused on the development of a method for determination of the local atomic structure of copper centers (specifically, a ring in the framework of copper-containing zeolite mordenite (Cu-MOR) in which copper atoms are located) that combines ML and XANES (X-ray absorption near edge structure) spectroscopy techniques.

1. Methods and approaches

An approach combining ML and XANES spectroscopy [20,21] with the use of synthetic data allows one not only to examine a large number of models of copper

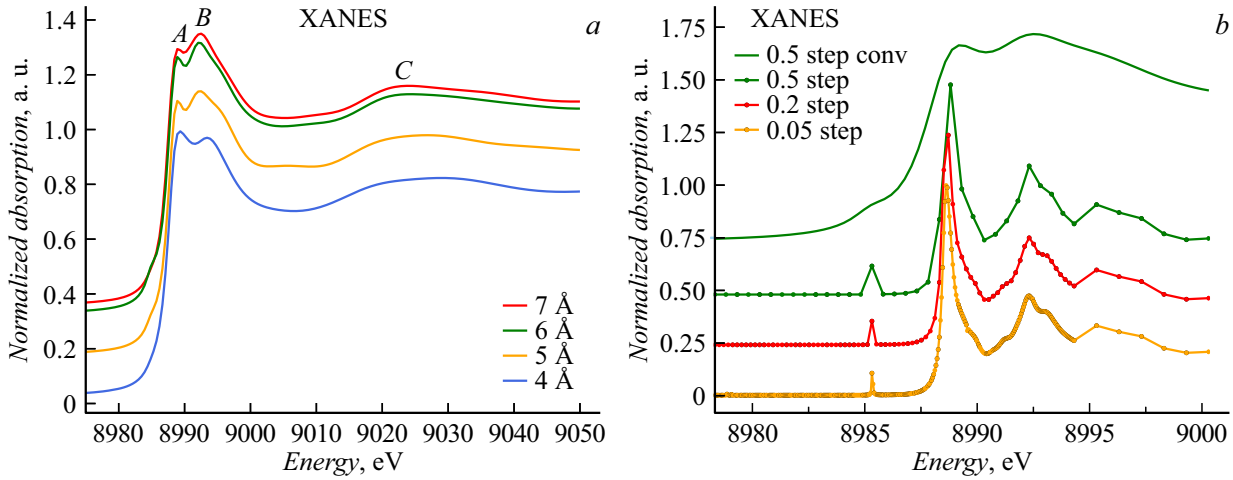

Figure 1. Theoretical Cu *K*-XANES spectra of the local environment of copper in the zeolite framework calculated for clusters of different sizes (*a*) and with different grid spacings near the absorption edge for a 6 Å cluster (*b*).

centers, but also to accelerate significantly the process of determination of structural parameters.

Classification, which is performed to divide data into classes and provides an opportunity to predict the result based on input data, is one of the objectives of machine learning. In the present case, zeolite framework rings containing copper atoms are the classes, and Cu *K*-XANES spectra of various Cu-MOR structures are the input data used for predictions. The procedure involves supervised training: a classifier is trained by providing it with structural models with already known rings containing copper centers and Cu *K*-XANES spectra values. This classifier may then be applied to experimental Cu *K*-XANES spectra and identify rings containing copper centers.

Structures were modeled with the use of the ASE (atomic simulation environment) library [22]. ASE is a software package written in Python with the aim of setting up, steering, and analyzing atomistic simulations. ASE provides modules for many standard simulation tasks, such as structure optimization and molecular dynamics. In the present study, models of copper centers are objects of the Atoms type (sets of atoms with given Cartesian positions). Geometric optimization was performed with the LAMMPS calculator from the ASE library with the use of the potential presented in [23].

Cu *K*-XANES spectra for various structural models of copper centers in Cu-MOR were calculated by the finite difference method implemented in FDMNES [24]. The finite difference method is a numerical technique for solving differential equations on a point grid. In the present case, the Schrödinger equation is solved for a spherical region around an absorbing atom that incorporates a cluster containing the needed number of atoms. Calculations for a cluster with a radius of 6 Å with a grid spacing of 0.5 Å near the absorption edge are sufficient to reproduce all key features of Cu *K*-XANES spectra of models of copper centers in Cu-MOR. The indicated cluster parameters were chosen after examining the influence of the corresponding parameters on the shape of theoretical Cu *K*-XANES spectra.

With the size of pores in the zeolite framework taken into account, calculations were performed for local copper environment clusters with a size of 4, 5, 6, and 7 Å. It was found that saturation of the theoretical Cu *K*XANES spectrum needed for classification of a copper center in the zeolite ring is observed when a cluster 6 Å in size is used: all key spectral features (A, B, C) for local copper environment in the Cu-MOR framework are reproduced in this case (Fig. 1, *a*). In addition, test calculations of Cu *K*-XANES spectra with different grid spacings (0.5, 0.2, and 0.05 Å) near the absorption edge were carried out. No significant changes in the shape of the theoretical spectrum were observed (Fig. 1, *b*). These calculations were performed in the excited state with the use of the Hedin–Lundqvist potential.

The UMAP (uniform manifold approximation and projection) method, which is one of the most advanced techniques for nonlinear dimension reduction and data visualization, was chosen to provide graphical representation of the set. This method relies on the concept of constructing a low-dimensional manifold that retains the topological structure of high-dimensional data; in other words, it conserves both the local nature of the distribution and the global structure of initial data [25].

2. Results and discussion

A training set containing Cu *K*-XANES spectra calculated in FDMNES for a set of models of copper centers positioned in different rings inside channels of the mordenite framework was formed in order to apply ML techniques to the problem of determination of the local atomic structure of Cu-MOR. Since zeolites have a complex aluminosilicate structure, we devised a naming convention for rings of the

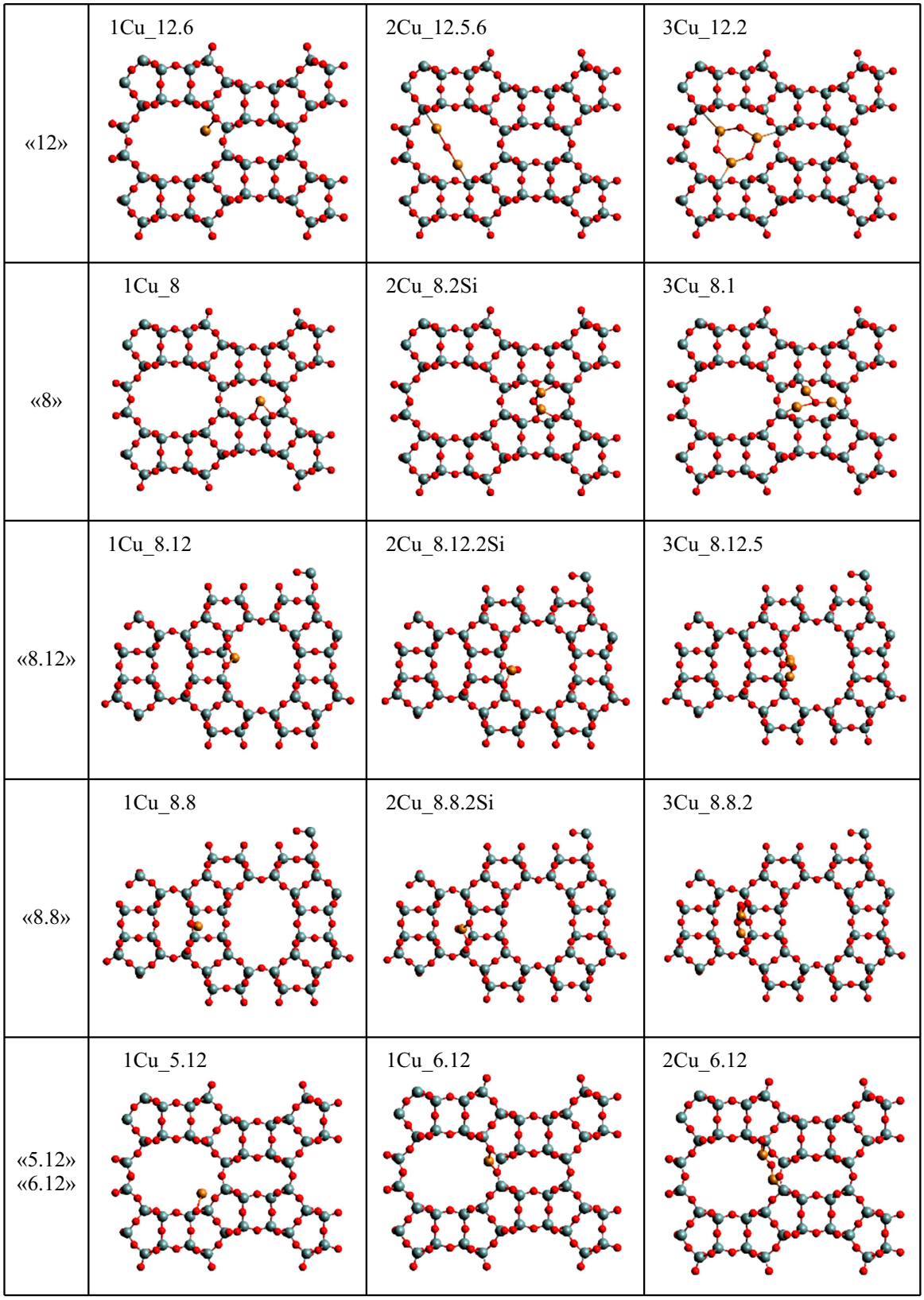

Figure 2. Schematic diagrams of certain models of copper centers in the Cu-MOR framework. The number of copper atoms is given before the designation of the primary class (e.g., 1Cu_12.6).

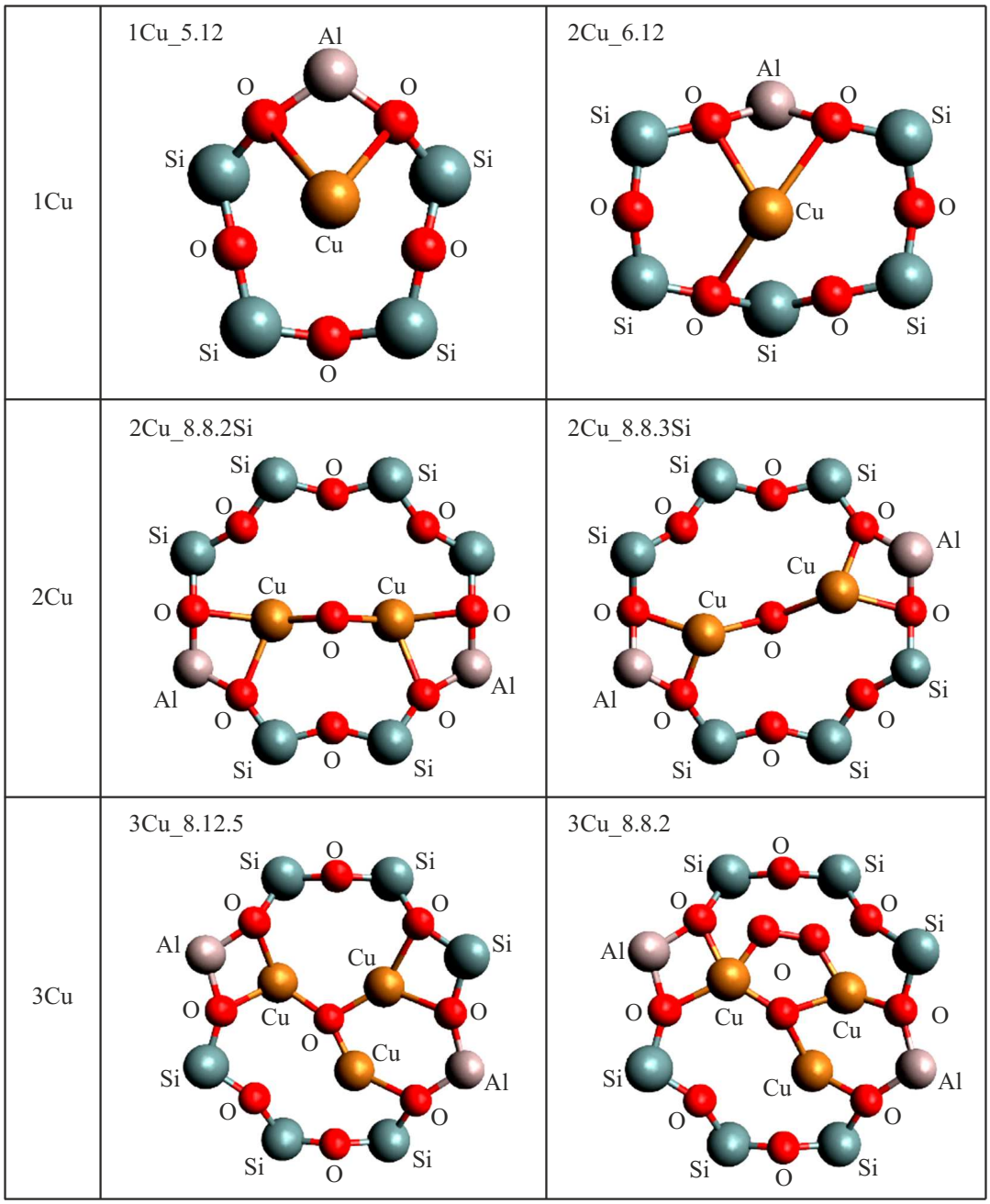

Figure 3. Schematic diagrams of certain rings in the Cu-MOR framework that allow for the formation of copper centers containing 1, 2, and 3 copper atoms, respectively.

Cu-MOR framework for convenience of interpretation of the obtained calculated data (Fig. 2).

A list of models was compiled based on the currently available literature data [26–28], where the most probable positioning of copper in the considered zeolite rings was taken into account. Figures 2 and 3 present the schematic models of copper centers located in different zeolite rings and containing 1, 2, or 3 copper atoms. Major classes of models were designated in accordance with the number of silicon atoms in a ring or channel in which copper atoms are located: „12“ — copper atoms are located in a 12-fold channel; „8“ — copper atoms are located in an 8-fold channel; „8.12“ and „8.8“ — copper atoms are located in an 8-fold ring that is an element of a 12- or 8-fold channel, respectively; and „5.12“ and „6.12“ — copper atoms are located in a 5- or 6-fold ring of a 12-fold channel.

These major classes were then divided into subclasses corresponding to different copper positions within a given principal class. Three subclasses („12.5,“ „12.6,“ and „12.8“) were chosen in class „12“ with one copper atom considered. The second index denotes the proximity to a certain ring in a 12-fold channel. Another three subclasses

Table 1. Designations of models in the training set for the neural network

Class	List of objects in this class		
12	12.5_1Cu, 12.6_1Cu, 12.8_1Cu	12.5.5_2Cu, 12.5.6_2Cu, 12.5.8_2Cu	12.1_3Cu, 12.2_3Cu, 12.3_3Cu
8	8_1Cu	8.2Si_2Cu, 8.3Si_2Cu	8.1_3Cu, 8.2_3Cu
8.12	8.12_1Cu	8.12.2Si_2Cu, 8.12.3Si_2Cu	8.12.1_3Cu, 8.12.2_3Cu, 8.12.3_3Cu, 8.12.4_3Cu, 8.12.5_3Cu, 8.12.6_3Cu
8.8	8.8_1Cu	8.8.2Si_2Cu, 8.8.3Si_2Cu	8.8.1_3Cu, 8.8.2_3Cu 8.8.3_3Cu, 8.8.4_3Cu, 8.8.5_3Cu, 8.8.6_3Cu
6.12	6.12_1Cu	6.12_2Cu	
5.12	5.12_1Cu		

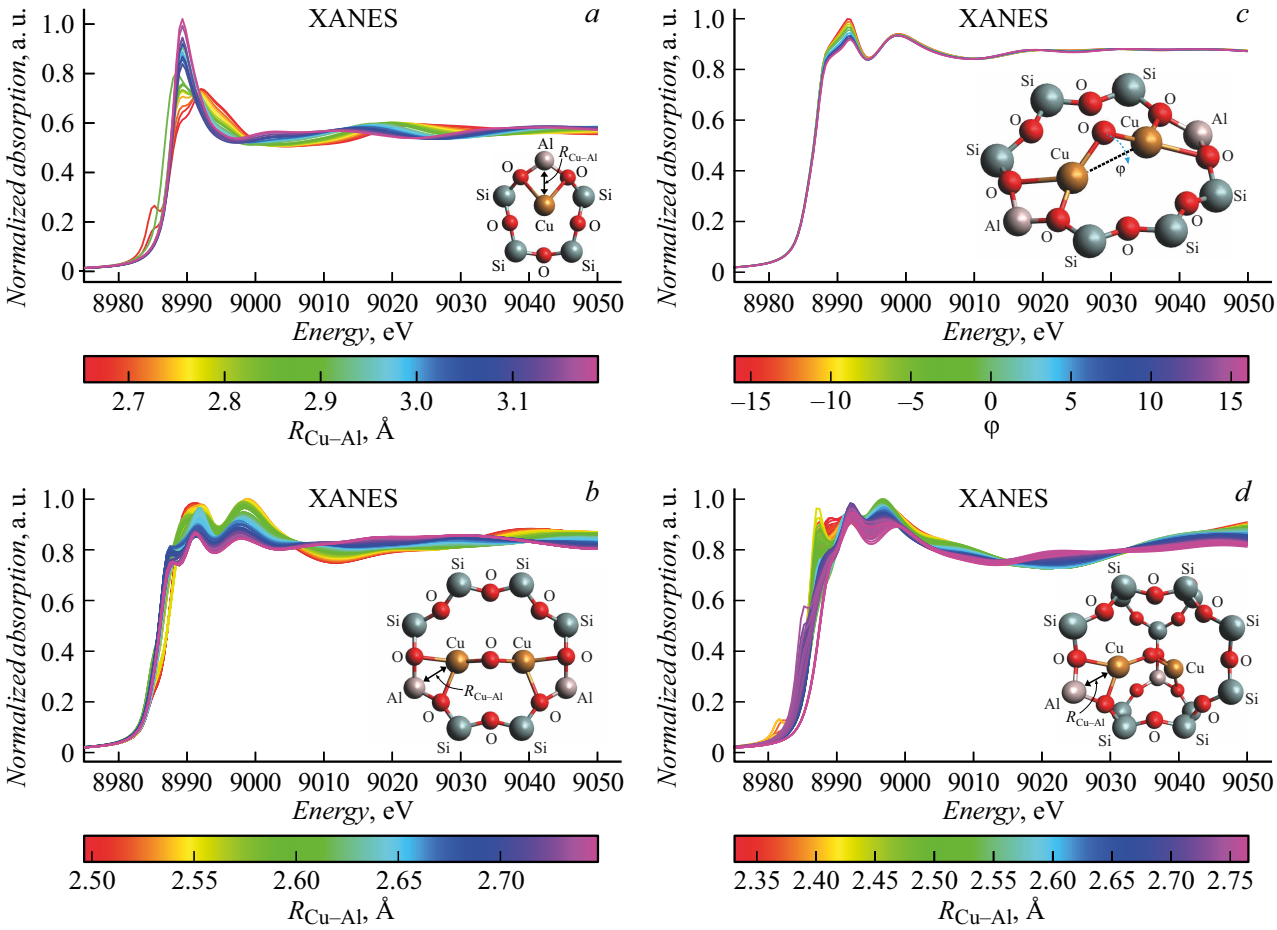

Figure 4. Calculated Cu *K*-XANES spectra for: the model of a copper center in ring 5.12 containing 5 oxygen atoms, 4 silicon atoms, and 1 aluminum atom (*a*); the model of a copper center in ring 8.8.2Si containing 8 oxygen atoms, 6 silicon atoms, and 2 aluminum atoms (*b*); the model of copper center 8.12.3Si in ring 8.12, where Cu-O-Cu chain rotation angle φ of 16° was varied with a pitch of 4° (*c*); and the model of copper center 8.3Si in ring 8 (*d*).

(„12.5.5," „12.5.6," and „12.5.8") were identified in the same class with two copper atoms considered. Figure 2 presents an example for model „12.5.6." Copper atoms in this model are bound to each other via an oxygen atom and to the framework via aluminum atoms found in 5- and 6-fold rings in a 12-fold channel. In a similar fashion, models

Table 2. Variation of structural parameters in the process of compilation of the database; $R_{\text{Cu-Al}}$ is the distance between copper and aluminum atoms and φ is the rotation angle

Cu	Model	Structural parameter	Parameter variation, $R_{\text{Cu-Al}}$, angstroms, and φ, degrees
1	12	$R_{\text{Cu-Al}}$	2.12−3.32
	12.6	$R_{\text{Cu-Al}}$	2.35−3.37
		$R_{\text{Cu-Al}}$	1.99−3.41
		$R_{\text{Cu-Al}}$	3.17−3.89
		$R_{\text{Cu-Al}}$	2.40−4.05
		$R_{\text{Cu-Al}}$	2.36−4.03
	6.12	$R_{1\,\text{Cu-Al}}$ $R_{2\,\text{Cu-Al}}$	2.51−3.15 2.53−3.42
	5.12	$R_{\text{Cu-Al1}}$ $R_{\text{Cu-Al2}}$ $R_{\text{Cu-Al3}}$	2.64−3.19 2.91−3.59 3.31−3.70
2	12.5.5	$R_{\text{Cu-Al}}$	2.12−3.32
	12.5.6	$R_{\text{Cu-Al}}$	1.92−3.12
	12.5.8	$R_{\text{Cu-Al}}$	2.29−3.49
	6.12	$R_{\text{Cu-Al}}$	1.82−2.82
	8.12.2Si	$R_{\text{Cu-Al}}$ φ	2.48−2.66 −16 − +16
	8.12.3Si	$R_{\text{Cu-Al}}$ φ	2.51−2.67 −16 − +16
	8.2Si	$R_{\text{Cu-Al}}$ φ	2.33−2.76 −16 − +16
	8.3Si	$R_{\text{Cu-Al}}$ φ	2.33−2.73 −16 − +16
	8.8.2Si	$R_{\text{Cu-Al}}$ φ	2.5−2.75 −16 − +16
	8.8.3Si	$R_{\text{Cu-Al}}$ φ	2.53−2.76 −16 − +16

for two copper atoms in rings „8,“„8.12,“ and „8.8“ were divided into two subclasses: „8.2Si,“ „8.3Si“; „8.12.2Si,“ „8.12.3Si“; and „8.8.2Si,“ „8.8.3Si“, where the number of silicon atoms in a ring between aluminum atoms is indicated (Fig. 3).

Three types of models differing in the positions of copper atoms in a ring and bonds via oxygen with each other and with the zeolite framework were considered for three copper atoms in channel „12“ „12.1,“„12.2,“and „12.3“. Similar designations were introduced for all the other models: models „8.1“ and „8.2“; „8.12.1,“ „8.12.2,“ „8.12.3,“ „8.12.4,“ „8.12.5,“ and „8.12.6“; and „8.8.1,“ „8.8.2,“ „8.8.3,“

Table 2 (*continued*).

Cu	Model	Structural parameter	Parameter variation, $R_{\text{Cu-Al}}$, angstroms, and φ, degrees
3	12.1	$R_{\text{Cu-Al}}$	3.73−4.04
	12.2	$R_{\text{Cu-Al}}$	3.73−4.04
	12.3	$R_{\text{Cu-Al}}$	3.34−3.69
	8.1	$R_{\text{Cu-Al}}$	3.37−3.91
	8.12.1	$R_{\text{Cu-Al}}$	2.03−2.55
	8.12.2	$R_{\text{Cu-Al}}$	2.25−2.73
	8.12.3	$R_{\text{Cu-Al}}$	2.03−2.55
	8.12.4	$R_{\text{Cu-Al}}$	2.03−2.55
	8.12.5	$R_{\text{Cu-Al}}$	2.03−2.55
	8.12.6	$R_{\text{Cu-Al}}$	2.03−2.55
	8.2	$R_{\text{Cu-Al}}$	3.62−4.12
	8.8.1	$R_{\text{Cu-Al}}$	1.81−1.92
	8.8.2	$R_{\text{Cu-Al}}$	2.36−2.53
	8.8.3	$R_{\text{Cu-Al}}$	1.81−1.92
	8.8.4	$R_{\text{Cu-Al}}$	1.81−1.92
	8.8.5	$R_{\text{Cu-Al}}$	1.81−1.92
	8.8.6	$R_{\text{Cu-Al}}$	2.47−2.56

„8.8.4,“ „8.8.5,“ and „8.8.6“ were considered for three copper atoms in channel „8“ and rings „8.12“ and „8.8,“ respectively.

Thus, the first and second numbers in designations for channels „12“ and „8“ (e.g., model „12.5“) denote the channel and the ring, respectively. These designations are necessary, since the position of a copper atom in the considered copper center varies along the channel. A different type of consecutive numbering, where the first and second numbers denote the ring and the channel to which this ring belongs, is used for other classes. In this case, the ring, which is the thought-for class, is the element of relevance. The designations of all classes in the set are listed in Table 1.

A data set including Cu *K*-XANES spectra for each model from the examined set with different varying structural parameters of the local environment of copper (interatomic distances $R_{\text{Cu-Al}}$ with account for different directions of displacement of a copper atom and rotation angle φ) was compiled for classifier training and testing (Fig. 4, *c*). The ranges of variation of structural parameters are listed in Table 2. The resulting data set consisted of 2100 calculated Cu *K*-XANES spectra for different models of copper centers. All non-equivalent positions of copper atoms were taken into account when introducing the resulting spectrum into the set.

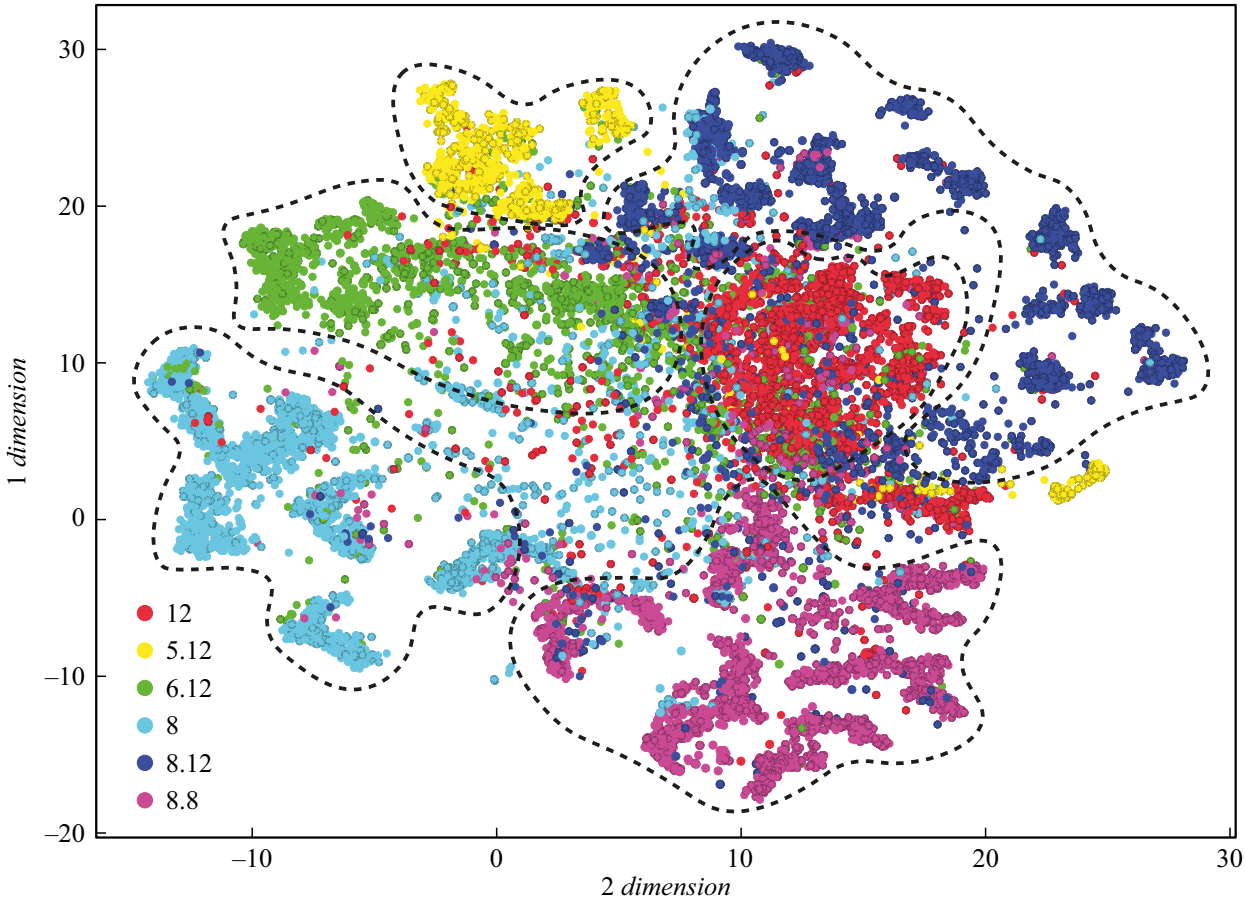

Figure 5. UMAP projection obtained with the use of Python umap for the set of Cu *K*-XANES data calculated for the models of copper centers in Cu-MOR. Different colors correspond to different rings containing a copper center (see the above naming convention and Fig. 1).

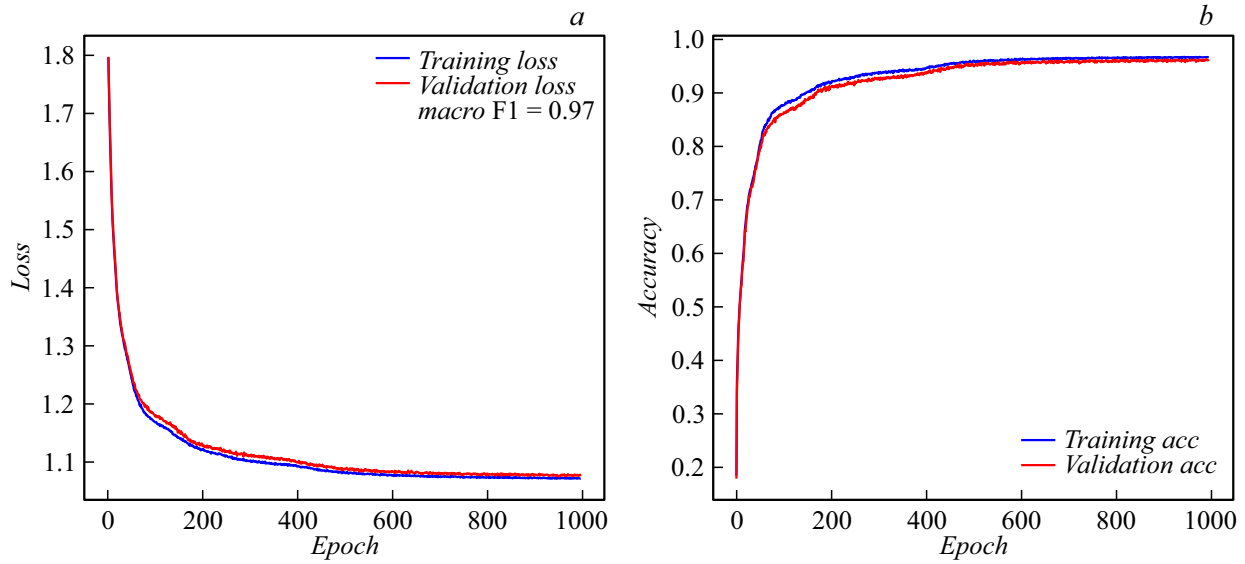

Figure 6. Loss function for the neural network. The number of epochs is plotted on axis OX, and the cross-entropy loss is plotted on axis OY (*a*). Accuracy metric for the neural network plotted in the course of training with the Cu *K*-XANES data set for Cu-MOR (*b*).

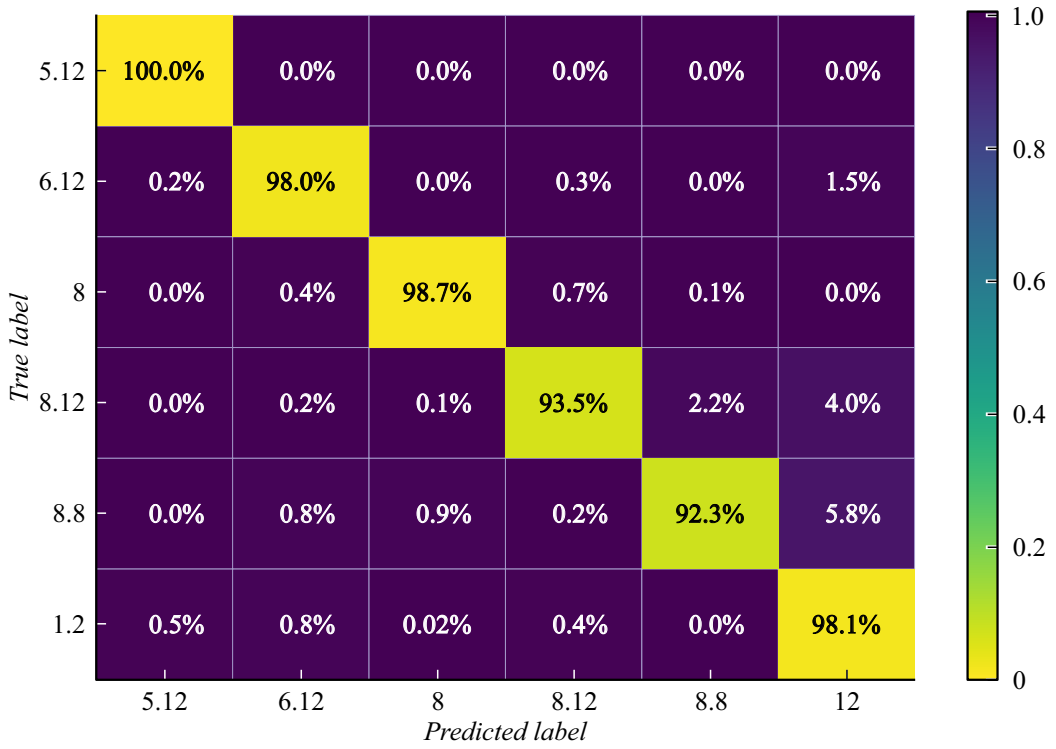

Figure 7. Normalized error matrix for the neural network trained on the training set of Cu *K*-XANES spectra for Cu-MOR. Rows are true classes, and columns are predicted classes. The error matrix was analyzed in order to identify the key difficulties in classification of certain specific attributes.

In addition, augmentation of theoretical data was performed with an allowance made for the influence of copper oxides (CuO and Cu_2O). With this aim in view, Cu *K*-XANES spectra formed as linear combinations of the considered models of copper centers and CuO and Cu_2O copper oxides with different contributions (25, 50, and 75% for each individual oxide) were added to the theoretical data set. Thus, the set consisted of 14700 theoretical Cu *K*-XANES spectra. Elements of the set for rings designated, in accordance with the above naming convention, as „5.12“ (Fig. 4, *a*), 8.8.2Si (Fig. 4, *b*), 8.12.3Si (Fig. 4, *c*), and 8.3Si (Fig. 4, *d*) are shown as examples in Fig. 4.

A neural network (MLP, multilayer perceptron) was chosen as a classifier, since it was found to be more accurate than such classical machine learning methods as Extra Trees Classifier, KNeighbors, and Random Forest, which had an accuracy of 0.80, 0.65, and 0.79, respectively, according to the F1 metric. Prior to training of the neural network, data were analyzed for the possibility of their clusterization by the UMAP nonlinear dimension reduction method. The reduction to two parameters made it possible to present the set in a graphic form (Fig. 5). With 100 neighbors and a minimum distance of 1, the data clearly group into clusters.

A fully connected neural network constructed based on pytorch modules [29] was used to identify the ring containing a copper center. The neural network consisted of an input linear layer, a dropout layer, a ReLU activation layer, a hidden linear layer, and a softmax layer. The dropout method nullifies certain elements of the input tensor with a probability of 0.25 with the use of samples from the Bernoulli distribution. The softmax function alters the input tensor in such a way so that its elements lie within the [0, 1] interval and add up to unity. The obtained output values may be regarded as approximate probabilities that an active copper center is positioned in given rings. Multiclass cross-entropy was used as a loss function. The test set was 33% of the entire data set. The Adam optimizer with a learning rate of 0.01 was used to perform training. The accuracy according to the F1 metric ceases to grow after 1000 epochs (training cycles) and stops at 96.6% for the test set and 97.4% for the training set (see Figs. 6, 7). It should be stressed that a model trained on non-augmented data, which is needed to exclude the possibility of finding similar spectra in training and test sets, was obtained at the first stage. The accuracy of the model was estimated by cross-validation with 10 subsets and was found to be 89% according to the average F1 metric. Thus, the model is statistically stable, and its accuracy is comparable to that of the model trained on augmented data.

The error matrix (Fig. 7) suggests that the neural network distinguishes fairly accurately (according to the F1 metric) between different structural zeolite rings. Diagonal elements represent the number of correctly classified rings of each class, while non-diagonal elements correspond to incorrectly classified rings.

Conclusion

An approach combining XANES spectroscopy, computer modeling, and ML was proposed to be used for determining the local atomic structure of copper centers formed in the Cu-MOR zeolite framework. Cu *K*-XANES spectra were calculated using the FDMNES software package for the obtained set of models of different types of copper centers. A proprietary naming convention for models of copper centers located in different rings of zeolite mordenite was proposed, and a training data set containing 14700 theoretical Cu *K*-XANES spectra (with the influence of CuO and Cu_2O oxides factored in) was compiled. The application of clusterization methods to the obtained model data revealed that Cu *K*-XANES spectra corresponding to the models of copper centers located in the same structural fragment are localized in the same region of the attribute space.

The feasibility of grouping attributes into clusters opens up opportunities for determination of the type of atomic structure (in particular, specific zeolite rings containing copper atoms) based on Cu *K*-XANES spectra. This potential was illustrated by training the neural network on theoretical spectra. The accuracy of the obtained characterization was rather high: 0.97 according to the F1 metric. In future studies, the constructed ML model will be applied in the analysis of experimental Cu *K*-XANES spectra.

Funding

This study was carried out with support from the Russian Science Foundation (grant No. 23-22-00438) at the Southern Federal University.

Conflict of interest

The authors declare that they have no conflict of interest.

References

[1] S.E. Bozbag, E.M.C. Alayon, J. Pecháček, M. Nachtegaal, M. Ranocchiari, J.A. van Bokhoven. Catal. Sci. Technol., **6**, 5011 (2016). DOI: 10.1039/C6CY00041J

[2] E.M.C. Alayon, M. Nachtegaal, A. Bodi, M. Ranocchiari, J.A. van Bokhoven. Phys. Chem. Chem. Phys., **17**, 7681 (2015). DOI: 10.1039/C4CP03226H

[3] E.M.C. Alayon, M. Nachtegaal, E. Kleymenov, J.A. van Bokhoven. Microporous Mesoporous Mater., **166**, 131 (2013). DOI: 10.1016/j.micromeso.2012.04.054

[4] B.F. Sels, L.M. Kustov (ed.). *Zeolites and Zeolite-Like Materials* (Elsevier, 2016), DOI: 10.1016/C2014-0-00257-2

[5] J.S. Woertink, P.J. Smeets, M.H. Groothaert, M.A. Vance, B.F. Sels, R.A. Schoonheydt, E.I. Solomon. Proc. Natl. Acad. Sci., **106**, 18908 (2009). DOI: 10.1073/pnas.0910461106

[6] V.V. Pryadchenko, G.B. Sukharina, A.M. Ermakova, S.V. Bazovaya, T.I. Kurzina, V.A. Durymanov, V.A. Tolstopyatenko, V.V. Srabionyan, L.A. Avakyan, L.A. Bugaev. Tech. Phys., **66**, 1018 (2021). DOI: 10.1134/S1063784221070124

[7] V.V. Srabionyan, G.B. Sukharina, S.Y. Kaptelinin, V.A. Durymanov, A.M. Ermakova, T.I. Kurzina, L.A. Avakyan, L.A. Bugaev. Phys. Solid State, **62**, 1222 (2020). DOI: 10.1134/S1063783420070252

[8] V.V. Srabionyan, G.B. Sukharina, T.I. Kurzina, V.A. Durymanov, A.M. Ermakova, L.A. Avakyan, E.M.C. Alayon, M. Nachtegaal, J.A. van Bokhoven, L.A. Bugaev. J. Phys. Chem. C, **125**, 25867 (2021). DOI: 10.1021/acs.jpcc.1c08240

[9] S. Grundner, M.A.C. Markovits, G. Li, M. Tromp, E.A. Pidko, E.J.M. Hensen, A. Jentys, M. Sanchez-Sanchez, J.A. Lercher. Nat. Commun., **6**, 7546 (2015). DOI: 10.1038/ncomms8546

[10] Q. Zhang, J. Yu, A. Corma. Adv. Mater., **32**, 2002927 (2020). DOI: 10.1002/adma.202002927

[11] A.A. Guda, S.A. Guda, A. Martini, A.L. Bugaev, M.A. Soldatov, A.V. Soldatov, C. Lamberti. Radiat. Phys. Chem., **175**, 108430 (2020). DOI: 10.1016/j.radphyschem.2019.108430

[12] A.A. Guda, S.A. Guda, A. Martini, A.N. Kravtsova, A. Algasov, A. Bugaev, S.P. Kubrin, L.V. Guda, P. Šot, J.A. van Bokhoven, C. Copéret, A.V. Soldatov. Npj Comput. Mater., **7**, 203 (2021). DOI: 10.1038/s41524-021-00664-9

[13] L. Avakyan, D. Tolchina, V. Barkovski, S. Belenov, A. Alekseenko, A. Shaginyan, V. Srabionyan, V. Guterman, L. Bugaev. Comput. Mater. Sci., **208**, 111326 (2022). DOI: 10.1016/j.commatsci.2022.111326

[14] M. Moliner, Y. Román-Leshkov, A. Corma. Acc. Chem. Res., **52**, 2971 (2019). DOI: 10.1021/acs.accounts.9b00399

[15] A. Gandhi, M.M.F. Hasan. Curr. Opin. Chem. Eng., **35**, 100739 (2022). DOI: 10.1016/j.coche.2021.100739

[16] J.D. Evans, F.-X. Coudert. Chem. Mater., **29**, 7833 (2017). DOI: 10.1021/acs.chemmater.7b02532.

[17] J.H. Friedman. Ann. Stat., **29**, 1189 (2001). DOI: 10.1214/aos/1013203451

[18] T. Hastie, J. Friedman, R. Tibshirani. *The Elements of Statistical Learning* (Springer, NY., 2001), DOI: 10.1007/978-0-387-21606-5

[19] Q. Zhu, Y. Gu, X. Liang, X. Wang, J. Ma. ACS Catal., **12**, 12336 (2022). DOI: 10.1021/acscatal.2c03250

[20] A.V. Soldatov, A.N. Kravtsova, L.N. Mazalov, S.V. Trubina, N.A. Kryuchkova, G.B. Sukharina. J. Struct. Chem., **48**, 1061 (2007). DOI: 10.1007/s10947-007-0171-0

[21] J.J. Rehr, A.L. Ankudinov. Coord. Chem. Rev., **249**, 131 (2005). DOI: 10.1016/j.ccr.2004.02.014

[22] A. Hjorth Larsen, J. Jørgen Mortensen, J. Blomqvist, I.E. Castelli, R. Christensen, M. Dułak, J. Friis, M.N. Groves, B. Hammer, C. Hargus, E.D. Hermes, P.C. Jennings, P. Bjerre Jensen, J. Kermode, J.R. Kitchin, E. Leonhard Kolsbjerg, J. Kubal, K. Kaasbjerg, S. Lysgaard, J. Bergmann Maronsson, T. Maxson, T. Olsen, L. Pastewka, A. Peterson, C. Rostgaard, J. Schiøtz, O. Schütt, M. Strange, K.S. Thygesen, T. Vegge, L. Vilhelmsen, M. Walter, Z. Zeng, K.W. Jacobsen. J. Phys. Condens. Matter, **29**, 273002 (2017). DOI: 10.1088/1361-648X/aa680e

[23] G.M. Psofogiannakis, J.F. McCleerey, E. Jaramillo, A.C.T. van Duin. J. Phys. Chem. C, **119**, 6678 (2015). DOI: 10.1021/acs.jpcc.5b00699

[24] Y. Joly. Phys. Rev. B, **63**, 125120 (2001). DOI: 10.1103/PhysRevB.63.125120
[25] M.S. Asyaky, R. Mandala. *Improving the Performance of HDBSCAN on Short Text Clustering by Using Word Embedding and UMAP*, in: 2021 8th Int. Conf. Adv. Informatics Concepts, Theory Appl., IEEE, (2021), p. 6. DOI: 10.1109/ICAICTA53211.2021.9640285
[26] B.E.R. Snyder, P. Vanelderen, R.A. Schoonheydt, B.F. Sels, E.I. Solomon. J. Am. Chem. Soc., **140**, 9236 (2018). DOI: 10.1021/jacs.8b05320
[27] M.H. Mahyuddin, T. Tanaka, A. Staykov, Y. Shiota, K. Yoshizawa. Inorg. Chem., **57**, 10146 (2018). DOI: 10.1021/acs.inorgchem.8b01329
[28] P. Han, Z. Zhang, Z. Chen, J. Lin, S. Wan, Y. Wang, S. Wang, Catalysts, **11**, 751 (2021). DOI: 10.3390/catal11060751
[29] Electronic source. Available at: https://pytorch.org/

Translated by D.Kondaurov